respectively

〈Superscripts〉

(0), (1), (i) = zeroth, first and i-th order terms in expansion respectively

—(overbar) = time-averaged value

Literature Cited

1) Carter, J. W. and M. L. Wyszynski: *Chem. Eng. Sci.*, **38**, 1093 (1983).
2) Chihara, K. and M. Suzuki: *J. Chem. Eng. Japan*, **16**, 53 (1983).
3) Chihara, K. and M. Suzuki: *J. Chem. Eng. Japan*, **16**, 293 (1983).
4) Gelbin, D., G. Bunke, H. J. Wolff and J. Neifess: *Chem. Eng. Sci.*, **38**, 1993 (1983).
5) Hassan, M. M., N. S. Raghvan, M. M. Ruthven and H. A. Boniface: *AIChE J.*, **31**, 2008 (1985).
6) Hirose, T. and T. Minoda: *J. Chem. Eng. Japan*, **19**, 300 (1986).
7) Hirose, T. and T. Minoda: *World Congress III of Chemical Engineering*, **2**, 825 (1986).
8) Kawai, T. (ed.): "Atsuryukusuingu Kyuchaku Gijutsushusei (Pressure Swing Adsorption)," Kogyogijutsukai, Tokyo, 1986.
9) Mitchell, J. E. and L. H. Shendalman: *AIChE Symp. Ser.*, **69**, No. 134, 25 (1973).
10) Raghavan, N. S., M. M. Hassan and D. M. Ruthven: *AIChE J.*, **31**, 385 (1985).
11) Shendalman, L. H. and J. E. Mitchell: *Chem. Eng. Sci.*, **27**, 1449 (1972).
12) Suzuki, M.: *AIChE Symp. Ser.*, **81**, No. 242, 67 (1985).
13) Underwood, R. P.: *Chem. Eng. Sci.*, **41**, 409 (1986).

(A part of this work was presented at the 51st Annual Meeting of The Society of Chemical Engineers, Japan at Osaka, 1986.)

FILTRATION CHARACTERISTICS OF MEMBRANES FOR PLASMA SEPARATION AND CHANGES IN MEMBRANE STRUCTURE AFTER BLOOD CONTACT

KIKUO OZAWA, RISHICHI MIMURA AND KIYOTAKA SAKAI

Department of Chemical Engineering, Waseda University, Tokyo 160

Key Words: Membrane Separation, Plasmapheresis, Microfiltration, Medical Chemical Engineering, Concentration Polarization, Solute Permeability

Plasma separation experiments with a hollow fibrous filter were made to clarify the effects of hematocrit, protein concentration and wall shear rate on filtrate flux. The resistance of the polarization layer caused by red blood cells is the dominant factor in filtration and accounts for 50 to 80% of total filtration resistance. Factors governing the filtrate flux in plasma separation are plasma viscosity, hematocrit and wall shear rate. An estimation equation for filtrate flux is proposed.

Membrane structural changes after plasma separation were evaluated to clarify fouling characteristics in plasma separation by using radioisotope-labeled solute and scanning electron microscopy. The decrease in pore diameter and surface porosity is attributed to both protein adsorption onto pore walls and plugging by red blood cells.

Introduction

Polymer membranes for therapeutic use in plasma separation show time-dependent decay in both filtrate flux and sieving coefficient during filtration.[3] Estimation of filtrate flux and sieving coefficient under various operating conditions is required in designing membranes for plasmapheresis. Mass transport phenomena in plasma separation cannot be explained by ultrafiltration theory since plasma separation is classified as microfiltration. Filtrate flux and sieving coefficient are influenced by operating conditions, module dimensions, membrane properties and blood properties. A relationship between filtrate flux and wall shear rate has been developed through analysis by modified filtration theory.[4,5,12]

The objective of the present study is to elucidate the effects of blood properties and operating conditions on filtrate flux, and to propose a mass transfer equation for estimating filtrate flux in plasma separation. Membrane structural changes after plasma separation were also evaluated to clarify fouling characteristics.

Received August 14, 1986. Correspondence concerning this article should be addressed to K. Sakai.

1. Experimental

1.1 Membrane

Technical data on the Plasmacure® PVA-SB hollow fibrous plasma separator (Kuraray, Osaka) tested in the present study are summarized in **Table 1**. The membrane material is polyvinyl alcohol. Both the inner diameter and wall thickness of hollow fiber membranes were measured by optical microscope under wet conditions. The volumetric water content indicated was determined with a pycnometer.[9]

1.2 Procedures

Figure 1 shows a schematic diagram of the experimental apparatus. Feed solutions of red blood cell suspension composed of bovine red blood cells in a physiological saline, bovine plasma and bovine blood were supplied to a filter through a roller pump at flow rates ranging from 0.83 to $2.50\times10^{-6}\,m^3\,s^{-1}$ ($\gamma_W=98$–$293\,s^{-1}$), at a transmembrane pressure of 2.0 kPa and a temperature of 310 K. The filtration experiments were made at protein concentrations ranging from 0 to $90\,kg\,m^{-3}$ and at hematocrits ranging from 0 to 50%.

Pure water permeability was measured first, then pure water was replaced with the feed solution, and the filtrate flux was measured after an hour. Pure water permeability was again measured after rinsing the filter with $2.0\times10^{-3}\,m^3$ of physiological saline. The protein adsorbing on membrane surfaces and within membrane pores was then fixed with 3% glutaraldehyde. Volumetric water content and solute permeability for radioisotope-labeled solute, ^{14}C-urea, were measured for native and treated membranes to evaluate structural changes after plasma separation.

Dialysis experiments for determining solute permeability were made at a dialysate velocity such that the boundary layer formed on the outside of the membrane tube could be completely eliminated. Data analysis of the time dependence of solute concentration remaining in the membrane tube is based on unsteady-state diffusion equations proposed by Stevenson.[8]

2. Results

2.1 Effects of protein concentration and hematocrit on filtrate flux

Figure 2 shows the effect of protein concentration on filtrate flux. Increasing protein concentration led to a decrease in filtrate flux. Filtrate flux was lower for blood than for plasma, because filtration resistance was higher with blood than with plasma.

The sieving coefficient for total proteins was over 0.98 and was stable with time in all experiments. Formed elements, mainly red blood cells, were not sieved by the membrane and were the dominant factor in filtration resistance. Filtrate flux, plotted as a function of hematocrit in **Fig. 3**, is found to decrease with increasing hematocrit. The mass balance of red blood cells in the polarization layer is represented[12] by

$$J_V=k\ln(Ht_W/Ht_B) \qquad (1)$$

where the mass transfer coefficient k and wall hematocrit Ht_W are calculated from the slope and intercept of the linear plots in Fig. 3.

Red blood cell suspension:

$$k=6.8\times10^{-7}\,m\,s^{-1}, \qquad Ht_W=230\%$$

Table 1. Technical data on Plasmacure® PVA-SB

Membrane material	Polyvinyl alcohol
Inner diameter $\times10^6$ [m]	346 ± 16*
Wall thickness $\times10^6$ [m]	115 ± 7*
Fiber length $\times10^2$ [m]	24.2
Number of fibers	2100
Membrane area [m^2]	0.55
Water content [$m^3\cdot m^{-3}$]	0.61
PWP [$m^3\cdot m^{-2}\cdot s^{-1}\cdot Pa^{-1}$]	4.58×10^{-9}

* Data taken under wet conditions and expressed in mean ± S.D. for 100 randomly chosen fibers.

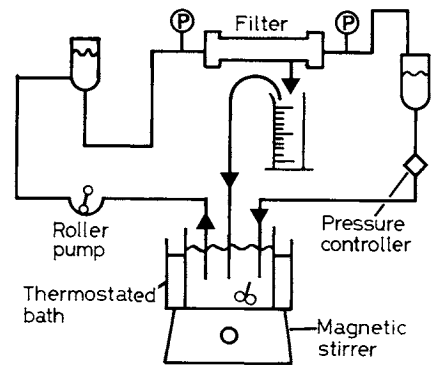

Fig. 1. Schematic diagram of experimental apparatus.

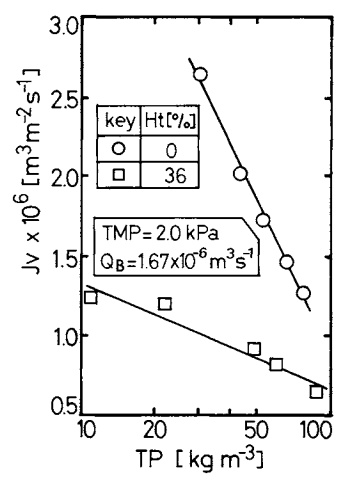

Fig. 2. Effect of protein concentration on filtrate flux.

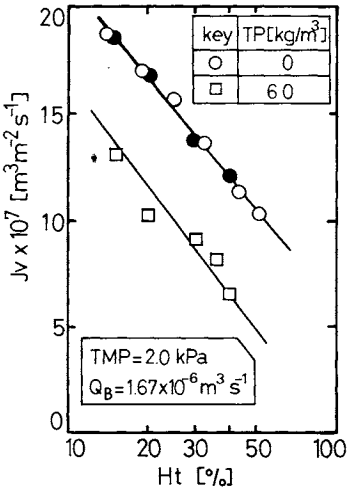

Fig. 3. Filtrate flux as a function of hematocrit. Closed plots indicate flux data as hematocrit is changed from 50 to 15%.

Blood:

$$k = 7.4 \times 10^{-7}\,\mathrm{m\,s^{-1}}, \qquad Ht_W = 95\%$$

Hysteresis on the filtrate flux-hematocrit relation was evaluated with red blood cell suspension. As can be seen from Fig. 3, no hysteresis is observed. The accumulation of red blood cells on membrane surfaces has been found to be reversible for red blood cell suspension.

2.2 Effects of wall shear rate on filtrate flux

Filtrate flux is plotted as a function of wall shear rate and hematocrit in **Figs. 4** and **5**. Filtrate flux and wall shear rate are linearly related on log-log plots. The slope is represented by the power term in the relationship $J_V \propto \gamma_W^{0.47}$. Values for the mass transfer coefficient and wall hematocrit calculated from the data in Fig. 5 are summarized in **Table 2**. It was found that wall hematocrit maintained a constant value of $95 \pm 7\%$ at varying wall shear rates and protein concentrations. Increasing protein concentration led to a decrease in the mass transfer coefficient because of an increase in viscosity. The mass transfer coefficient increased with wall shear rate because of enhanced back-diffusion of red blood cells.

2.3 Quantitative changes in membrane parameters after plasma separation

The effects of protein concentration and hematocrit on quantitative changes in three membrane parameters —solute permeability for ^{14}C-urea, pure water permeability and water content— before and after blood contact are summarized in **Table 3**. Filtration experiments were made at a blood flow rate of $1.67 \times 10^{-6}\,\mathrm{m^3\,s^{-1}}$ and a transmembrane pressure of 2.0 kPa. Solute permeability, pure water permeability and water content decreased with increasing protein concentration. The decrease from the values for native membranes associated with increasing hematocrit

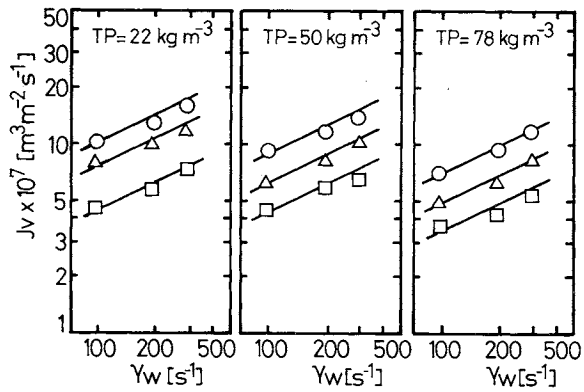

Fig. 4. Filtrate flux as a function of wall shear rate. Q_B: $1.67 \times 10^{-6}\,\mathrm{m^3 \cdot s^{-1}}$. *TMP*: 2.0 kPa. *Ht*: ○, 24.5%; △, 35%; □, 50%.

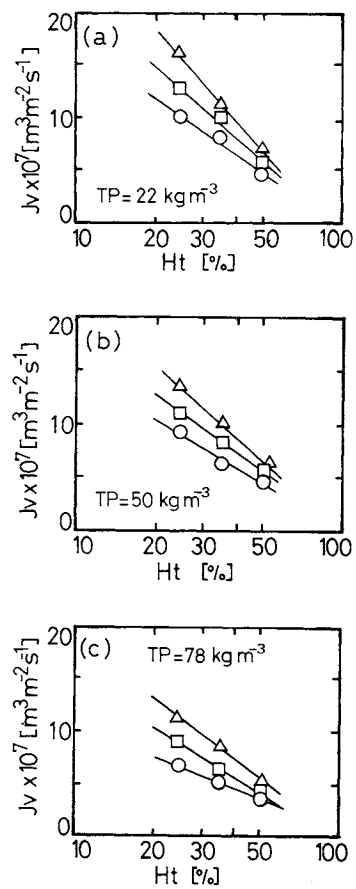

Fig. 5. Filtrate flux as a function of hematocrit. (a) $TP = 22\,\mathrm{kg \cdot m^{-3}}$; (b) $TP = 50\,\mathrm{kg \cdot m^{-3}}$; (c) $TP = 78\,\mathrm{kg \cdot m^{-3}}$. *TMP*: 2.0 kPa. γ_w: ○, $98\,\mathrm{s^{-1}}$; □, $195\,\mathrm{s^{-1}}$; △, $293\,\mathrm{s^{-1}}$.

from 15 to 40% were 20–35% for solute permeability, 40–50% for pure water permeability and 10–30% for water content. The quantitative changes in these parameters were higher after blood contact than after plasma contact. **Figure 6** shows a scanning electron micrograph of membrane surfaces after plasma separation at a wall shear rate of $98\,\mathrm{s^{-1}}$, a transmembrane pressure of 2.0 kPa, a protein concentration of $74\,\mathrm{kg/m^3}$ and a hematocrit of 38%. Microscopic

Table 2. Calculated values for mass transfer coefficient and wall hematocrit

TP [kg·m^{-3}]	$k\times10^7$ [m·s^{-1}]			Ht_W [%]		
	$\gamma_W=98\,s^{-1}$	$\gamma_W=195\,s^{-1}$	$\gamma_W=293\,s^{-1}$	$\gamma_W=98\,s^{-1}$	$\gamma_W=195\,s^{-1}$	$\gamma_W=293\,s^{-1}$
22	7.65	9.98	12.7	94	91	86
50	6.38	7.60	10.3	99	106	92
78	4.58	6.97	8.24	105	85	98

Table 3. Experimental results on solute permeability, pure water permeability and water content before and after plasma separation

(a) $Ht=0\%$

TP [kg·m^{-3}]	$Pm\times10^6$ [m·s^{-1}]	$PWP\times10^9$ [m^3·m^{-2}·s^{-1}·Pa^{-1}]	H [m^3·m^{-3}]
30	2.99 (7)	4.22 (8)	0.58 (5)
43	2.90 (10)	3.94 (14)	0.56 (8)
52	2.89 (11)	3.92 (15)	0.54 (12)
66	2.82 (13)	3.78 (18)	0.54 (12)
78	2.77 (14)	3.59 (22)	0.52 (15)

(b) $Ht=36\%$

TP [kg·m^{-3}]	$Pm\times10^6$ [m·s^{-1}]	$PWP\times10^9$ [m^3·m^{-2}·s^{-1}·Pa^{-1}]	H [m^3·m^{-3}]
11	2.31 (29)	3.53 (23)	0.44 (28)
22	2.30 (29)	3.27 (29)	0.44 (28)
50	2.26 (30)	2.64 (42)	0.43 (30)
60	2.23 (31)	2.40 (48)	0.43 (30)
86	2.16 (33)	1.88 (59)	0.42 (31)

(c) $TP=60\,kg\,m^{-3}$

Ht [%]	$Pm\times10^6$ [m·s^{-1}]	$PWP\times10^9$ [m^3·m^{-2}·s^{-1}·Pa^{-1}]	H [m^3·m^{-3}]
15	2.83 (19)	2.66 (42)	0.55 (10)
20	2.61 (20)	2.54 (45)	0.50 (18)
30	2.35 (27)	2.48 (46)	0.45 (26)
36	2.23 (31)	2.38 (48)	0.43 (30)
40	2.15 (34)	2.29 (50)	0.41 (33)

Native membrane: $Pm=3.23\times10^{-6}$ m/s; $PWP=4.58\times10^{-9}$ m^3·m^{-2}·s^{-1}·Pa^{-1}; $H=0.61$.
Figures in parentheses refer to reduction percentage for treated membranes compared to native membranes.

observation demonstrates that red blood cells are deposited in the pores.

3. Discussion

3.1 Filtration resistance

Filtrate flux J_V may be represented by

$$J_V=TMP/(R_M+R_A+R_P) \tag{2}$$

$$R_M=1/PWP_{PRE} \tag{3}$$

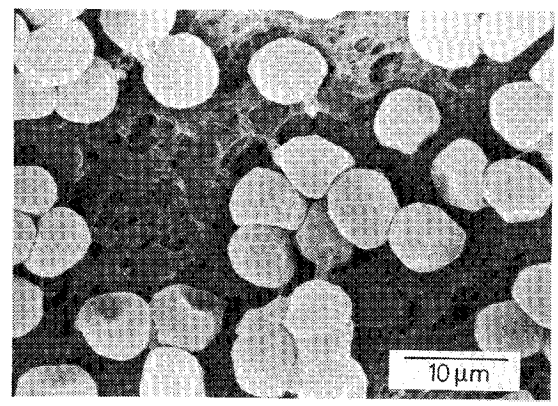

Fig. 6. Scanning electron micrograph of membrane after plasma separation.

$$R_A=1/PWP_{POST}-R_M \tag{4}$$

$$R_P=(1/LP_{PLASMA})(\mu_W/\mu_P)-R_M-R_A \tag{5}$$

where R_M is the resistance of the membrane, R_A that of the irreversible adhesion layer, and R_P that of the polarization layer. **Figures 7** and **8** show the effects of protein concentration and hematocrit respectively on filtration resistance. R_A with plasma is less than 25% of R_M, while R_P is 150 to 260% of R_M. At a constant hematocrit of 36%, R_A increased with protein concentration because of an increase in plasma viscosity. R_P did not vary significantly with protein concentration at constant hematocrit and accounted for 80% of total filtration resistance. As Fig. 8 shows, increasing hematocrit leads to a rapid increase in R_P, while R_A keeps constant at varying hematocrits. R_A for red blood cell suspension was negligible. The major resistance to filtrate flux was found to come from the polarization layer formed by red blood cells. R_A was about the same as R_M and made only a minor contribution to the decline in filtrate flux.

3.2 Structural changes in membranes before and after plasma separation

A tortuous pore model[7] is proposed in which tortuosity is introduced into pore model.[10] The tortuous pore model allows determination of pore diameter D_P, surface porosity A_k and tortuosity τ from data on water content, solute and pure water permeability. The reduction percentage in pore diameter and surface porosity after plasma separation is shown in **Fig. 9** as a function of protein concentration and

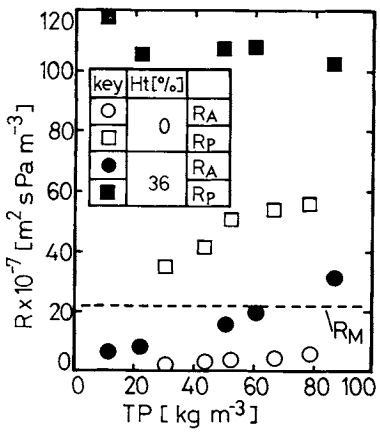

Fig. 7. Effect of protein concentration on filtration resistance. Q_B: $1.67\times10^{-6}\,m^{-3}\cdot s^{-1}$. *TMP*: 2.0 kPa.

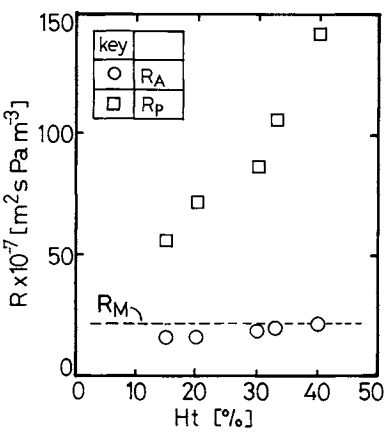

Fig. 8. Effect of hematocrit on filtration resistance. Q_B: $1.67\times10^{-6}\,m^3\cdot s^{-1}$. *TMP*: 2.0 kPa. *TP*: $60\,kg\cdot m^{-3}$.

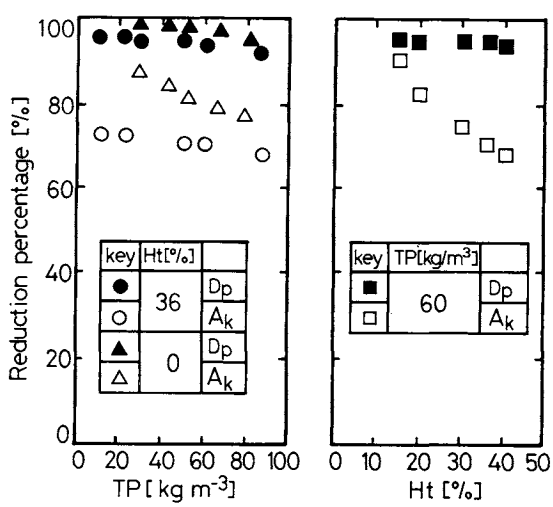

Fig. 9. Reduction percentage on pore radius and surface porosity of membrane after plasma separation. Native membrane: $D_P=3130\times10^{-10}$ m; $A_k=0.3$.

hematocrit. It seems that tortuosity maintains a constant value. Protein adsorption on pore walls decreases pore diameter and red blood cell deposition causes pore plugging. The pore diameter exhibits a drop of 40 to 160×10^{-10}m, and this corresponds to the size of one or more protein molecules. This shows that one or more layers of protein adsorb on pore walls.[6]

Membrane pores are plugged rapidly in the presence of protein and red blood cells, and increases in protein concentration and hematocrit lead to increased pore plugging. Pore plugging by red blood cells is affected by blood properties and operating conditions.

The diameter of red blood cells is larger than that of pores. Pores near those plugged by red blood cells are plugged simultaneously as shown in Fig. 6. The decrease in pore diameter and surface porosity after plasma separation is attributed to both the reduction in pore diameter resulting from protein adsorbing on pore walls and the decrease in the number of pores resulting from red blood cells plugging into membrane pores. The ratio of the number of red blood cells in blood in a single membrane tube to the number of pores on membrane surfaces is 1 : 10 with a hematocrit of 0.4, while the fact that red blood cells cause pore plugging indicates accumulation of red blood cells on membrane surfaces. This suggests that the red blood cell polarization model is a reasonable one in explaining the transport phenomena during plasma separation.

3.3 Estimation of filtrate flux

As previously described, the effect of hematocrit on filtrate flux is given by Eq. (1). The mass transfer coefficient k in ultrafiltration is represented by Blatt[1] as

$$k=B(D^2\gamma_W/L)^{1/3} \tag{6}$$

The diffusivity of red blood cells and other particles is dependent on wall shear rate. Eckstein[2] has reported the diffusivity of disk or spherical particles with varying radii at varying volumetric fractions as expressed by Eq. (7).

$$D=0.025a^2\gamma_W \tag{7}$$

Using a Couette electrolytic cell, Wang[11] has reported Eq. (8) representing the dependence of the diffusivity of red blood cells on wall shear rate.

$$D\propto\gamma_W^{0.9} \tag{8}$$

Substituting Eqs. (6) and (7) into Eq. (1), Zydney and Colton have proposed an estimation equation of filtrate flux for a plate-type plasma separator.[12]

$$J_V=0.07(a^4/L)^{1/3}\gamma_W\ln(Ht_W/Ht_B) \tag{9}$$

Jaffrin[4] has reported that filtrate flux was proportional to $\gamma_W^{0.74}$ using a similar analysis for a hollow-fiber plasma separator.

The average value of wall hematocrit of 95% obtained from the experimental results in Table 2 is in

good agreement with the value obtained by Zydney and Colton.[12]

The mass transfer coefficient increased with wall shear rate and with decreasing protein concentration. These observations suggest that the diffusivity of red blood cells is dependent not only on wall shear rate but also on protein concentration. **Figure 10** shows the relationship between mass transfer coefficient and wall shear rate. The closed plots in Fig. 10 indicate the mass transfer coefficient corrected for viscosity, $k(\mu_p/\mu_w)$. The mass transfer coefficient was calculated as a function of these factors as

$$k = 1.0 \times 10^{-5}(\mu_w/\mu_p)\gamma_W^{0.47} \qquad (10)$$

Substituting Eq. (10) into Eq. (1), we obtained

$$J_V = 1.0 \times 10^{-5}(\mu_w/\mu_p)\gamma_w^{0.47} \ln(Ht_W/Ht_B) \qquad (11)$$

Equation (11) gives filtrate flux at varying wall shear rates from 98 to 293 s^{-1}, at varying hematocrits from 25 to 50% and at varying protein concentrations from 22 to 78 kg/m^3.

Conclusion

Plasma separation experiments were made at various values of hematocrit, protein concentration and wall shear rate to elucidate the fouling characteristics of membranes. The resistance of the polarization layer caused by red blood cells is the dominant factor in filtrate flux. Surface porosity and pore diameter apparently decrease after plasma separation. SEM observation shows that pore plugging is caused mainly by red blood cells. Pore plugging is markedly exacerbated by the interaction between red blood cells and protein. The diffusivity of red blood cells is obtained as a function of wall shear rate and viscosity. An equation for estimating filtrate flux is proposed.

Acknowledgment

The authors would like to express their thanks for a part of the financial support for this study from the Waseda University Grant for Special Research Projects. They are also indebted to Mr. Shingo Yamane of the Tokyo-Tokatsu Clinic, Chiba, Japan for help and advice in analytical procedures concerning radioisotope-labeled solutes.

Nomenclature

A_k	=	surface porosity	[—]
a	=	radius of red blood cell	[m]
D	=	diffusivity	$[m^2 \cdot s^{-1}]$
H	=	water content	$[m^3 \cdot m^{-3}]$
Ht	=	hematocrit	[%]
J_V	=	filtrate flux	$[m^3 \cdot m^{-2} \cdot s^{-1}]$
k	=	mass transfer coefficient	$[m \cdot s^{-1}]$
L	=	length	[m]
Pm	=	solute permeability	$[m \cdot s^{-1}]$
PWP	=	pure water permeability	$[m^3 \cdot m^{-2} \cdot s^{-1} \cdot Pa^{-1}]$
Q	=	flow rate	$[m^3 \cdot s^{-1}]$

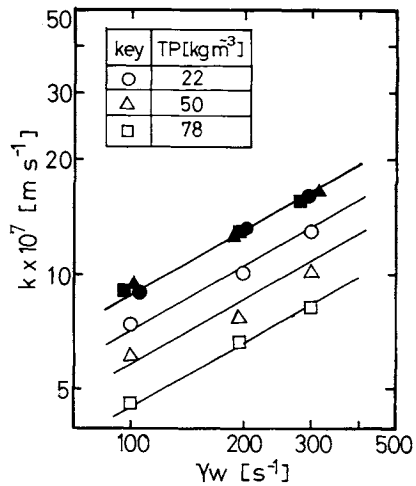

Fig. 10. Mass transfer coefficient as a function of wall shear rate and protein concentration. Closed plots indicate calculated values of mass transfer coefficient corrected for viscosity.

R_A	=	resistance of irreversible adhesion layer	$[m^2 \cdot s \cdot Pa \cdot m^{-3}]$
R_M	=	resistance of membrane	$[m^2 \cdot s \cdot Pa \cdot m^{-3}]$
R_P	=	resistance of polarization layer	$[m^2 \cdot s \cdot Pa \cdot m^{-3}]$
TMP	=	transmembrane pressure	[Pa]
TP	=	protein concentration	$[kg \cdot m^{-3}]$
γ_W	=	wall shear rate	$[s^{-1}]$
μ_p	=	plasma viscosity	[Pa·s]
μ_w	=	viscosity of water	[Pa·s]
τ	=	tortuosity	[—]

〈Subscripts〉

B	=	blood
$PLASMA$	=	during plasma separation
$POST$	=	after plasma separation
PRE	=	before plasma separation
W	=	membrane wall

Literature Cited

1) Blatt, W. F., A. Dravid, A. S. Michaels and L. Nelson: "Membrane Science and Technology," ed. by J. E. Flinn, p. 47, Plenum Press, New York (1970).
2) Eckstein, E. C., D. G. Bailey and A. H. Shapiro: *J. Fluid Mech.*, **79**, 191 (1977).
3) Friedman, L. I., R. A. Hardwick, J. R. Daniels, R. R. Stromberg and A. A. Ciarkoski: *Artif. Organs*, **7**, 435 (1983).
4) Jaffrin, M. Y., B. B. Gupta, L. H. Ding and M. Garreau: *Trans. Am. Soc. Atrif. Intern. Organs*, **30**, 401 (1984).
5) Malbrancq, J. M., M. Y. Jaffrin, E. Bouveret, R. Angleraud and G. Vantard: *asaio J.*, **7**, 16 (1984).
6) Matsuda, T., H. Takano, K. Hayashi, Y. Taenaka, S. Takaichi, M. Umezu, T. Nakamura, H. Iwata, T. Nakatani, T. Tanaka, S. Takatani and T. Akutsu: *Trans. Am. Soc. Artif. Intern. Organs*, **30**, 353 (1984).
7) Sakai, K., S. Takesawa, R. Mimura and H. Ohashi: *J. Chem. Eng. Jpn.*, **20**, 351 (1987).
8) Stevenson, J. F., M. A. Von Deak, M. Weinberg and R. W. Schuette: *AIChE J.*, **21**, 1192 (1975).
9) Takesawa, S., S. Oumi, Y. Konno, K. Sakai, M. Sekiguchi, S. Shimokoshi and T. Takahashi: *Jpn. J. Artif. Organs*, **15**, 1346 (1986).

10) Verniory, A., R. Du Bois, P. Decoodt, J. P. Gassee and P. P. Lambert: *J. Gen. Physiol.*, **62**, 489 (1973).
11) Wang, N. H. L. and K. H. Keller: *Trans. Am. Soc. Artif. Intern. Organs*, **25**, 14 (1979).
12) Zydney, A. L. and C. K. Colton: *Trans. Am. Soc. Artif. Intern. Organs*, **28**, 408 (1982).

(Presented in part at the 51st Annual Meeting of The Society of Chemical Engineering, Japan, at Osaka, March 1986.)

STRUCTURAL ANALYSIS OF HOLLOW FIBER DIALYSIS MEMBRANES FOR CLINICAL USE

KIYOTAKA SAKAI, SHINGO TAKESAWA, RISHICHI MIMURA AND HIDEHIKO OHASHI

Department of Chemical Engineering, Waseda University, Tokyo 160

Key Words: Dialysis Membrane, Pore Radius, Solute Permeability, Pure Water Permeability, Surface Porosity, Tortuosity, Water Content

Little is known of the structure of hollow-fiber dialysis membranes for clinical use or of the effects of structure on solute and pure water permeability. Knowledge of such aspects of membrane structure as pore radius, surface porosity, tortuosity and water content is required if the desired membranes are to be designed.

The objective of the present study, therefore, is to obtain data on the pore radius, surface porosity and tortuosity of hollow-fiber dialysis membranes through an analysis of measured water content, and of solute and pure water permeability on the basis of a newly introduced tortuous pore model. In regenerated cellulose membranes, pore radius ranges from 21 to 34×10^{-10} m, and huge pores ranging in radius from 47 to 64×10^{-10} m are identified for EVA membranes which are permeable to small amounts of serum protein. Values for surface porosity of the regenerated cellulose and EVA membranes are approximately 33 and 22%, and tortuosity is approximately 1.9 and 2.2, respectively. The tortuous pore model combined with the L_p and P_m method is well suited for elucidating the relationship between membrane structure and solute and pure water permeability.

Introduction

The performance of currently utilized hemodialyzers is absolutely dependent on the permeability of their membranes. Appropriate design of dialysis membranes requires correct values for pore radius, surface porosity, water content and tortuosity. It has proved impossible to find the pore radius of dialysis membranes using the mercury porosimeter or electron microscope because the pores are only several tens of angstroms in radius. Consequently, indirect procedures such as the L_p method that uses both pure water permeability and water content,[1] the L_p and P_m method, which uses both pure water and solute permeability[4,5,7,8] and the σ method that uses the reflection coefficient[3,8,14] have been employed extensively. Structural data obtained from the procedures referred to above may lack reliability, however, because those procedures depend on a simplified pore model that assumes that membrane pores are formed perpendicular to the membrane surface.

The objective of the present study is to obtain data on the pore radius, surface porosity and tortuosity of hollow-fiber dialysis membranes through an analysis of measured water content, and of solute and pure water permeability on the basis of a newly introduced tortuous pore model.

1. Theoretical

Kedem and Katchalsky[2] derived phenomenological transport equations based on nonequilibrium thermodynamics. In this analysis, membrane characteristics are expressed as three transport parameters—reflection coefficient, and solute and pure water permeability. The membrane is considered to be a black box.

The simplified pore model[7] directly relating membrane structure to these transport parameters was improved by Verniory[13] and Kimura[6] with tortuosity omitted in any pore model. Qualitative attempts to account for tortuosity in the pore model have been successful.[9]

Received October 1, 1986. Correspondence concerning this article should be addressed to K. Sakai.